ACS SENSORS

Subscriber access provided by UNIVERSITY OF SOUTH CAROLINA LIBRARIES

Article

Crossed Surface Relief Gratings as Nanoplasmonic Biosensors

Srijit Nair, Carlos Escobedo, and Ribal Georges Sabat

ACS Sens., **Just Accepted Manuscript** • DOI: 10.1021/acssensors.6b00696 • Publication Date (Web): 17 Feb 2017

Downloaded from http://pubs.acs.org on February 19, 2017

Just Accepted

"Just Accepted" manuscripts have been peer-reviewed and accepted for publication. They are posted online prior to technical editing, formatting for publication and author proofing. The American Chemical Society provides "Just Accepted" as a free service to the research community to expedite the dissemination of scientific material as soon as possible after acceptance. "Just Accepted" manuscripts appear in full in PDF format accompanied by an HTML abstract. "Just Accepted" manuscripts have been fully peer reviewed, but should not be considered the official version of record. They are accessible to all readers and citable by the Digital Object Identifier (DOI®). "Just Accepted" is an optional service offered to authors. Therefore, the "Just Accepted" Web site may not include all articles that will be published in the journal. After a manuscript is technically edited and formatted, it will be removed from the "Just Accepted" Web site and published as an ASAP article. Note that technical editing may introduce minor changes to the manuscript text and/or graphics which could affect content, and all legal disclaimers and ethical guidelines that apply to the journal pertain. ACS cannot be held responsible for errors or consequences arising from the use of information contained in these "Just Accepted" manuscripts.

ACS Publications

ACS Sensors is published by the American Chemical Society. 1155 Sixteenth Street N.W., Washington, DC 20036

Published by American Chemical Society. Copyright © American Chemical Society. However, no copyright claim is made to original U.S. Government works, or works produced by employees of any Commonwealth realm Crown government in the course of their duties.

Crossed Surface Relief Gratings as Nanoplasmonic Biosensors

Srijit Nair,[1] Carlos Escobedo[1,] and Ribal Georges Sabat[2,*]*

[1]Department of Chemical Engineering, Queen's University, 19 Division St., Kingston, Ontario K7L 3N6, Canada

[2]Department of Physics, Royal Military College of Canada, Kingston, Ontario K7K 7B4, Canada

ABSTRACT

We present an original, low-cost nanoplasmonic (bio)sensor based on crossed surface relief gratings (CSRGs) generated from orthogonally superimposed surface relief gratings (SRGs) on gold-coated azo-glass substrate. This surface plasmon resonance (SPR)-based sensing approach is unique, since the light transmitted through a CSRG is zero except in the narrow bandwidth where the SPR conversion occurs, enabling quantitative monitoring of, only, the plasmonic signal from bio-molecular interactions in real-time. We validated the individual SRG plasmonic signature of CSRGs by observing their respective SPR excitation peaks, and tested them to detect both bulk and near-surface refractive index (RI) changes. Compared to simple SRGs, CSRGs portray a much-improved sensitivity of 647.8 nm/RIU, a resolution in the order of 10^{-5} RIU, and a figure of merit (FOM) of 14 for bulk RI-change sensing. We also demonstrate their ability to perform as biosensors, through the detection and monitoring of near-surface bio-molecular interactions in real-time, a first for CSRGs. The minimum detectable concentration of biotin-streptavidin binding events was 8.3 nM. Due to their sensing abilities, low-cost (<10 cents/unit), easiness of fabrication and inherent suitability for integration with microfluidics, we anticipate that CSRGs will stand as strong candidates in the portable diagnostics arena.

KEYWORDS: nanophotonics, metallic nanostructure, surface plasmon resonance, surface relief grating, biosensing.

Nanostructured metallic films that support surface plasmon resonance (SPR) have been used as (bio)sensors in numerous applications in medicine and life sciences in the past few years.[1–6] Specific applications of SPR-based biosensing that can be found in the literature include detection of contaminants in food and water,[7–10] immunoassays,[11] DNA-protein interactions[12] and detection and monitoring of antigen-antibody binding events in real time.[13,14] Among the wide repertoire of metallic nanostructures available to date, surface relief gratings (SRGs) offer key advantages for biosensing applications requiring in-situ or portable detection due to their inherent compact footprint, compatibility with collinear optical formats and easiness of integration with other micro-technological platforms, such as microfluidics.[15–17] SRGs offer sensitivities compatible with biomedical diagnostics, precise and nanofabrication-based tunable SP excitations, and the possibility of performing real-time detection of analytes at very low fabrications and operation cost. [18,19] Additionally, the plasmonic signal from SRGs can be acquired in transmission-mode settings, minimizing alignment and assembly requirements.

The inscription of SRGs on azopolymer thin films has been around for more than two decades.[20] This nanofabrication phenomenon takes advantage of the unique photomechanical properties of the azobenzene chromophores, where a repetitive *trans* to *cis* photoisomerization occurs in the material under laser light illumination. In turn, optical nano-structures can be photo-inscribed in the azo film mimicking a laser interference pattern. This macroscopic phenomenon occurs due to the mass transport of the azo molecules from regions of high laser irradiance towards regions of lower irradiance. Typical linear SRGs are written using a simple Lloyd mirror where half of a collimated laser beam is incident on a mirror at right angle with an azo thin film. The grating's pitch is dependent on the laser incidence angle, while its depth is related to the laser exposure time.[21] This single-step fabrication process allows the inscription of

SRGs on a large scale in only a few minutes. Furthermore, a second exposure of a linear SRG to the writing laser under a different orientation permits the inscription of a second superimposed SRG, while retaining the diffraction effects of both gratings. After coating with a metallic layer, the azo nano-structures will be retained and SPR can be excited at the metal/dielectric interface above the SRGs when a diffracted order is phase-matched to the SPR wave vector. For a single linear SRG, this resonance will occur only when a probe light beam polarization is oriented along the grating vector.[22] Also, the SPR wave vector (hence the SPR wavelength) is dependent on parameters such as the SRG pitch, refractive indices (RIs) of the metal and the dielectric and the light incidence angle. In a wavelength scan, at normal incidence and for light polarization along to the SRG vector, the SPR on a linear grating is seen as a sharp positive peak in transmission, several times the original transmitted light intensity.[23] This occurs due to an enhanced transparency of the metal layer caused by the resonant electrons.

SPR propagation on perpendicular bi-gratings has shown that a polarization conversion of the incident light occurs.[24,25] When linearly polarized light is incident on a bi-grating, a SPR will be excited by the grating having a vector aligned with the initial light polarization. In turn, this SPR resonant light will be re-radiated by the crossed grating in its orthogonal polarization. Other studies have been done on the angular dependence of this SPR polarization conversion in azobenzene crossed SRGs and the results of light momentum transfer in between the gratings were explained in terms of the 2-dimensional SPR wave vectors.[26,27] This SPR approach in crossed SRGs (CSRGs) is remarkable since, when placed in between crossed polarizers, light transmitted through a CSRG will be zero except in the narrow bandwidth where the SPR conversion has occurred.

Here, we present a novel biosensing approach that takes advantage of the remarkably low cost, functionality and superior sensing abilities of plasmonic CSRGs. Based on a 6 mm x 6 mm sensor, coated with 60 nm of gold, a total production time of 10 min and a facility usage fee of $8/h, the fabrication cost is estimated at $0.09 USD per sensor. The resulting cost-effective and easy-to-fabricate device allows sensing in transmission mode and with the aid of minimal optics, making it suitable for point-of-care and other applications requiring portability. We demonstrate that the CSRG-based biosensor has superior sensitivity compared to established SRG-based sensors, and enables the detection of bio-molecular near-surface interactions, a first for CSRGs.

MATERIALS AND METHODS

Fabrication Methods.

Azo-glass. Disperse Red 1 (1.00 g, 3.18 mmol) in dry THF (10 ml) was slowly added to a stirred suspension of N,N'-carbonyldiimidazole (0.773 g, 4.77 mmol) in dry THF (5 ml) in a dry round-bottomed flask equipped with a magnetic stirrer at ambient temperature. The mixture was then stirred for 18 hours under N_2 atmosphere. The mixture was then separated into organic and aqueous layer by addition of CH_2Cl_2 and H_2O. The organic layer was washed two more times with copious amounts of H_2O and later recovered, dried over Na_2SO_4, filtered, and the solvent was evaporated. The crude residue was then dissolved in THF (15 ml) and 2-methylamino-4-mexylamino-6-(2-aminoethylamino)- 1,3,5-triazine (1.10 g, 3.82 mmol) was added. This mixture was then refluxed for 18 hours and later, the solvent was evaporated. 1M aq. HCl was then added to it and the precipitate was collected by filtration. The precipitate was then washed with 1 M aq. HCl and H_2O until the effluent was colorless. This residue was then dissolved in acetone and CH_2Cl_2 and aq. $NaHCO_3$ were added to separate the organic and aqueous layers. The organic

layer was dried over Na_2SO_4, filtered, and the volatiles were thoroughly evaporated under reduced pressure to yield 1.875 g of DR1-glass (2.99 mmol, 94%).[28]

DR1-glass film deposition. A solution of DR1-glass (3 wt%) in CH_2Cl_2 was prepared and mechanically shaken for 1 hour, then sieved via a 50 μm syringe filter (EMD Millipore, Merck KGaA, Darmstadt, Germany). A thin film of DR1-glass was then deposited using a Headway Research spin-coater. Approximately 3 ml of the solution was deposited on a BK7 glass slide with dimensions of 3 × 3 cm^2, at a rate of 1000 RPM for 20 seconds. The films were then dried in a Yamato ADP- 21 oven at 95^0C for 1 hour. Film thicknesses were measured with a Sloan Dektak II surface profiler (Veeco Instruments Inc., Plainview, NY, USA).

CSRGs fabrication. A solid-state diode-pumped laser (COHERENT, USA, Verdi V5, λ = 532 nm) with an irradiance of 382 mW/cm^2 was used for holographic exposure to create the SRGs. A DR1-glass coated sample was irradiated by two interfering beams from the laser, one directly incident, one reflected upon a 3 × 3 cm^2 Lloyd mirror placed orthogonally to the sample. The circularly polarized incident beam was collimated, and passed through a variable iris with a 1 cm diameter opening, which yielded SRGs with a grating area of approximately 0.39 cm^2. The grating pitch of the CSRGs was controlled via an in-house-built rotating sample holder assembly, by fine-tuning the angle of incidence of the laser on the sample. Details on the fabrication method of SRGs can be found elsewhere.[17] For this work, metal deposition was performed using a Bal-Tec SCD 050 sputter coater to deposit 60-nm-thick Au film in an Ar chamber (I = 50 mA, t = 150 secs).

Sensing Experiments. A PDMS layer of 2 mm in thickness was prepared by mixing Sylgard 184 elastomer and curing agent (Dow Corning, Midland, MI) at a 10:1 ratio, as detailed elsewhere.[18] An opening of 2 mm × 2 mm was carved onto a 1 cm × 1 cm piece of cured PDMS

and was placed atop the crossed region of the CSRGs. A stock solution of 20% (w/v) sucrose solution in deionized water was prepared for preparing the test solutions (5%, 10% and 20% sucrose solutions) used in the experiments. The RIs of the test samples were measured using an Abbe refractometer (Shanghai Optical Instruments, China).

Spectral Analysis. Origin™ Pro 8.0 software (OriginLab Corporation, USA) was used to perform the spectral analysis of the acquired SPR signals. The acquired spectra were normalized, plotted and fitted using GaussAmp fit in Origin ($R^2 > 0.9$). FOM was calculated from the sensitivity value obtained and the full-width half maximum (FWHM) of the raw fitted data, represented by:

$$FOM = (Sensitivity/FWHM) \quad (1)$$

Biosensing Experiment. For the biosensing experiment, the surface of the CSRGs was rinsed with 10% acetone and ultrapure water, and then plasma-cleaned for 15 minutes. A single-well (2 mm × 2 mm) PDMS layer was placed atop the clean crossed region of the CSRGs to host the analyte solutions over the surface. The opening was incubated with 5.18 mM cysteamine solution (Sigma-Aldrich, Canada) for 72 hours at room temperature. Next, the CSRGs were cleaned with 10% ethanol and deionized water to remove unbound cysteamine remnants. PBS was next added to the PDMS well and the transmission spectrum was recorded. The wavelength of the SPR peak was used as baseline for measuring the peak-shifts in the subsequent binding experiments. An NHS-terminated biotin residue solution (NHS-biotin, Sigma-Aldrich, Canada) with a concentration of 24.56 mM in PBS was then poured onto the CSRGs and incubated for 1 hour. The sample was then rinsed with PBS and the resulting transmission spectrum was recorded to verify the SPR peak-shift due to biotin adsorption. The biotin-modified CSRGs were then incubated in a streptavidin PBS solution (Sigma-Aldrich, Canada) at 0.83, 8.3, 83, 830 nM

in concentration, and the transmission spectra were recorded over time. For the single concentration (830 nM) biosensing experiment, the transmission spectra from the CSRGs were collected in real time, every minute. For the dose-dependence study, the spectra were acquired every 10 min. for a total of 120 minutes.

RESULTS AND DISCUSSION

Nanofabrication. Fig. 1a shows the fabrication process of the CSRGs using laser-inscription. First, powders of photoactive azo-glass (DR1-glass) were dissolved in dichloromethane and thoroughly mixed.[28] Subsequently, cleaned BK7 glass substrates were spin coated using the azo-glass solution to produce uniform films. The thickness of the films is controlled via the azo-glass solution concentration and the spin-coating rate. Since azo-glass solid films have an absorbance maximum around 485 nm, the deposition of thick films would result in increased absorption of light when operating in transmission mode while, in contrast, very thin films result in gratings being too shallow to generate strong surface plasmons.[28] For this reason, the thickness of the azo-glass film for each test sample was measured using a laboratory-grade profilometer and optimized for this experiment, resulting in a thickness of ca. 190 nm. In order to further eliminate any absorption effects from the azo-glass layer in transmission mode, the SRGs were inscribed with a pitch that would generate surface plasmons in the wavelength region where azo-glass is almost completely transparent (above 600 nm). Surface plasmons can be excited at the surface between a metal and a dielectric when the surface plasmon wave number k_{sp} given by:

$$k_{sp} = k_0 n\left(\sqrt{\varepsilon_m/(n^2 + \varepsilon_m)}\right) \quad (2)$$

where k_0 is the light wave number in free space, n is the index of refraction of the dielectric, and ε_m is the real part of the permittivity of the metal, is phased-matched to the grating vector given by:

$$k_{sp} = k_0 n \sin\theta \pm 2\pi m/\Lambda \quad (3)$$

where θ is the incidence angle, m is an integer and Λ is the grating pitch.[27] At normal incidence, equating equations (1) and (2) allows solving for the light wavelength where the surface plasmon occurs (λ_{SPR}), which is given by:

$$\lambda_{SPR} = n\Lambda\left[\sqrt{\varepsilon_m/(n^2+\varepsilon_m)}\right] \quad (4)$$

Based on a pitch of 550 nm, for an air/Au interface, a theoretical λ_{SPR} of 610 nm can be obtained. Using these input parameters, a first 550-nm-pitch linear SRG was laser-inscribed using a laser irradiance of 382 mW/cm^2 on the DR1-glass thin film by direct holographic exposure for 300 seconds. The substrate was then rotated 90 degrees and exposed to the laser beam for an additional 60 seconds to create a second perpendicularly superimposed 550-nm-pitch SRG atop the first SRG, as shown in Fig. 1a, resulting in the final CSRGs. This double exposure resulted in orthogonal gratings having nearly identical depths, which equates to nearly similar diffraction efficiencies. The surface of the CSRGs was then coated with a 60-nm-thick Au film using sputtering deposition. It is worth mentioning that the specific characteristics of the individual SRGs, such as the grating pitch and depth, can be precisely controlled within the unit of nanometer accuracy range, by simply changing the fabrication settings: laser power, exposure time and angular position of the sample. The surface profile of the fabricated CSRGs was investigated using AFM, which confirmed the successful creation of cross-grating patterns with the desired pitch and a depth of ca. 75 nm. Fig. 1b shows an actual picture of the resulting CSRGs and Fig. 1c shows an AFM image of the topography of a CSRG.

CSRGs Optical Characterization. Fig. 2 shows the schematics of the experimental setup used for the optical characterization of the CSRGs. A 12 V, 50 watts, halogen lamp was used as a light source, held in a horizontal position by a custom-made mount. Two Wollaston linear polarizers were used to polarize the light in horizontal and vertical directions respectively. A custom-made holder was used to orient the CSRGs orthogonally to the incident halogen light beam and a separate holder was used to position the spectrometer fiber optic tip for maximum signal capture. All the components were positioned in a linear arrangement atop an optical rail. The white light from the halogen lamp was first directed through the horizontally aligned polarizer and then onto the metallic bi-gratings. At this stage, a surface plasmon is first excited at the metal-dielectric interface above the CSRG, by the single grating component having its peaks and troughs along the vertical. An SPR energy exchange then occurs between this first grating and its orthogonal counterpart having its peaks and troughs along the horizontal. This SPR energy is then re-radiated by the second grating, as explained elsewhere.[26] The resulting out-coupled light then passes through the second linear polarizer, with its axis along the vertical, hence eliminating all residual light from the halogen lamp, except the light that passed through the SPR polarization conversion process. Recall that for single linear SRGs, only incident light polarized in the direction of the grating vector can couple into SPR.[26] Since CSRGs consist of two perpendicularly superimposed linear SRGs, a validation was done to verify if the CSRGs still retained the individual SRGs characteristics. The (second) polarizer positioned behind the sample was removed and the resulting transmission spectrum of the crossed-region of a CSRG was obtained when the first polarizer was set to transmit vertically (Fig. 3a) and then to transmit horizontally (Fig. 3b). These spectra were normalized to light transmitted through an area of the

sample where there was no grating. The SPR peaks observed in both light polarizations show the plasmons excited from each linear grating component. The difference in the SPR peak intensity can be correlated to a slight difference in the depth of each individual SRG. An optimized setup could be arranged to have perfectly identical depths for the crossed gratings, but this is not required and of minimal importance for the significance of this work. Next, the second linear polarizer was re-mounted and set to transmit horizontally, while the first polarizer was set to transmit vertically, and the resulting transmission spectrum from within the crossed-region of the CSRGs was obtained. The spectrum was normalized by the transmission spectrum of a flat gold/azo-glass area for establishing a comparative measure with respect to the signal from single SRGs. Fig. 3c shows the normalized SPR peak for the crossed-region for the CSRGs. The resulting peak was much sharper, although with a small decrease in its relative intensity, as compared to the individual SRGs signal obtained for the crossed-region of CSRGs. Both of these observations can be associated with the truncation of the residual light by the second polarizer. The loss of intensity is also due to the absorption of some of the light by the second polarizer.

Bulk Refractive Index Change Sensing. The CSRGs were first tested for the detection of changes in bulk refractive indices. A polydimethylsiloxane-siloxane (PDMS) layer with a single opening of 2 mm by 2 mm atop the crossed region of the CSRGs was used to expose the nano-structures to liquids with different RIs. The test solutions used in these experiments were deionized water, and aqueous sucrose solutions of 5%, 10% and 20% in concentration (w/v) with respective RIs of 1.330, 1.337, 1.344 and 1.357. The transmitted spectrum of the light passing through the CSRGs for each solution was acquired using the experimental setup described previously. Fig. 4a shows the SPR peaks corresponding to each solution and red peak-shift

associated with the change in bulk RI. The acquired SPR signals were processed and the total peak-shift at 90% maximum intensity was recorded. The total peak-shift, as a function of the RI, exhibited a linear increase as shown in Fig. 4b. The sensitivity of the CSRGs, obtained from the linear fit shown in this figure, was 647.8 nm/RIU, which represents a 3-fold improvement, compared to sensitivity values reported in the literature for SRGs sensing in transmission mode.[29] The resolution of the CSRGs was estimated to be in the order of 10^{-5} RIU, based on a measured standard deviation of 10^{-2} nm, and the calculated sensitivity.[30] This value is particularly important since resolution is typically used as a measure of efficacy in optical sensing as it takes the system noise into account. We have hypothesized before and confirm with this experiment that the significant increase in sensitivity is due to the plasmonic light transfer in the CSRG and the exclusion of all other wavelengths from the light source passing through the two polarizers. The calculated figure of merit (FOM) of the sensor was 14, which is comparable to other nanostructured SPR-based sensor technologies that require expensive nanofabrication methodologies or complex experimental setups.[31–33]

Biosensing Test. Motivated by the high sensitivity achieved for bulk RI changes, we investigated the utility of CSRGs as biosensing platforms for the detection of near-surface bio-molecular interactions. It is worth mentioning that this experiment represents the first demonstration of CSRG-based biosensing. A biotin-streptavidin system was used as receptor-analyte system as the binding kinetics of this complex is established and abundantly reported in the literature for proof-of-concept biosensing testing. Additionally, this bio-molecular system is suitable for characterizing biosensing testing as it has low dissociation constant, in the order of 10^{-14} M, and the time required to reach a quasi-steady binding state can be estimated based on

first-order Langmuir kinetics.[34,35] Fig 5a shows a schematic representation of the assembly of the biotin-streptavidin complex that has been built onto the surface of a CSRG via a cysteamine self-assembled monolayer (SAM) as anchoring molecule. A detailed description of the methodology is provided in the methods section. Fig 5b shows the measured peak-shift as a result from streptavidin binding to biotin on the surface of the CSRGs during incubation. The sharp and nearly linear peak-shift increase between times t = 3 min. and t = 14 min. correspond to the streptavidin initial binding to the surface, dominated by the on-kinetics. For the times t > 14 min, the quasi-steady state between the streptavidin and biotin is demonstrated by nearly constant peak wavelength. In contrast, the plateau after 20 min. demonstrates that quasi-steady state has been reached, in which binding is regulated by both on- and off-kinetics. The total peak-shift at the end of the biotin-streptavidin binding process was 2.67 nm. The inset in Fig. 5b shows the SPR peak-shifts corresponding to the binding events of cysteamine-biotin and biotin-streptavidin complexes using cysteamine as signal baseline. As the efficacy of any sensor is limited by the availability of the analyte (i.e. the analyte concentration), we performed a dose-based binding study to determine the minimum concentration of streptavidin detectable by the CSRGs. The experiment was carried out using new, identical CSRGs, and the previously described cysteamine-biotin complex formation protocol. Four streptavidin solutions with concentrations of 0.83, 8.3, 83 and 830 nM were used in this experiment. Fig. 5c shows the SPR peak-shifts corresponding to biotin-streptavidin binding over time for the four different concentrations. The minimum detectable streptavidin concentration, in this experiment, was 8.3 nM of streptavidin. It is noticeable that the test involving the 8.3 nM streptavidin solution did not reach a plateau for the length assigned for this experiment (120 minutes). However, a detectable signal at this concentration was clearly observed. It is also worth mentioning that the SPR peak-shifts

observed in this experiment are consistent with studies reported previously in the literature.[36–38] Most importantly, these results validate the utility of CSRGs as biosensing platform.

CONCLUSION

This work highlights the first experimental demonstration of both CSRGs-based sensing and biosensing. A transmission-based optical assembly was established for SPR polarization conversion in CSRGs with the help of two crossed/cancelling polarizers. We presented that CSRGs, retaining their individual SRG diffraction characteristics, provide a major improvement in sensitivity (647.8 nm/RIU, FOM - 14) compared to traditional SRGs. We also verified the CSRGs' ability to detect local refractive index changes with a surface modification study using streptavidin-biotin assay, aimed at projecting CSRGs as (bio)sensors. One of the drawbacks encountered while working with the CSRGs is their limit in working with corrosive solvents since azo-glass degrades upon interaction with strong solvents, causing damage to the nano-structures of the SRGs. However, this problem can be mitigated by transferring the CSRG pattern from the azo film to another substrate through soft lithography[39] or by photo-embossing.[40] But, from the prospect of sensing biological molecules, azo-glass CSRGs should not be a problem in lieu of the non-corrosive nature and near physiological pH of solvents used for biological analysis. The CSRGs sensors are extremely appealing because they are cost-effective, facile to fabricate and can be easily scaled-up for high-throughput applications. Also, since CSRGs are essentially superimposed SRGs, they can also be used in reflection or angular scan setups, depending upon the desired application. In the future, further improvement in the sensing assembly can be accomplished by integration of CSRGs into a microfluidic platform providing rapid, better-controlled and automated setup.

AUTHOR INFORMATION

Corresponding Authors

*E-mail: (R.G.S.) sabat@rmc.ca

*E-mail: (C.E.) carlos.escobedo@chee.queensu.ca

Author Contributions

The manuscript was written through contributions of all authors. All authors have given approval to the final version of the manuscript. S.N., C.E. and R.G.S. contributed equally.

Notes

The authors declare no competing financial interest.

ACKNOWLEDGMENT

This work was supported by the Natural Sciences and Engineering Research Council (NSERC) Discovery Grants and the Canada Foundation for Innovation (CFI) John R. Evans Leader Fund programs.

FIGURES

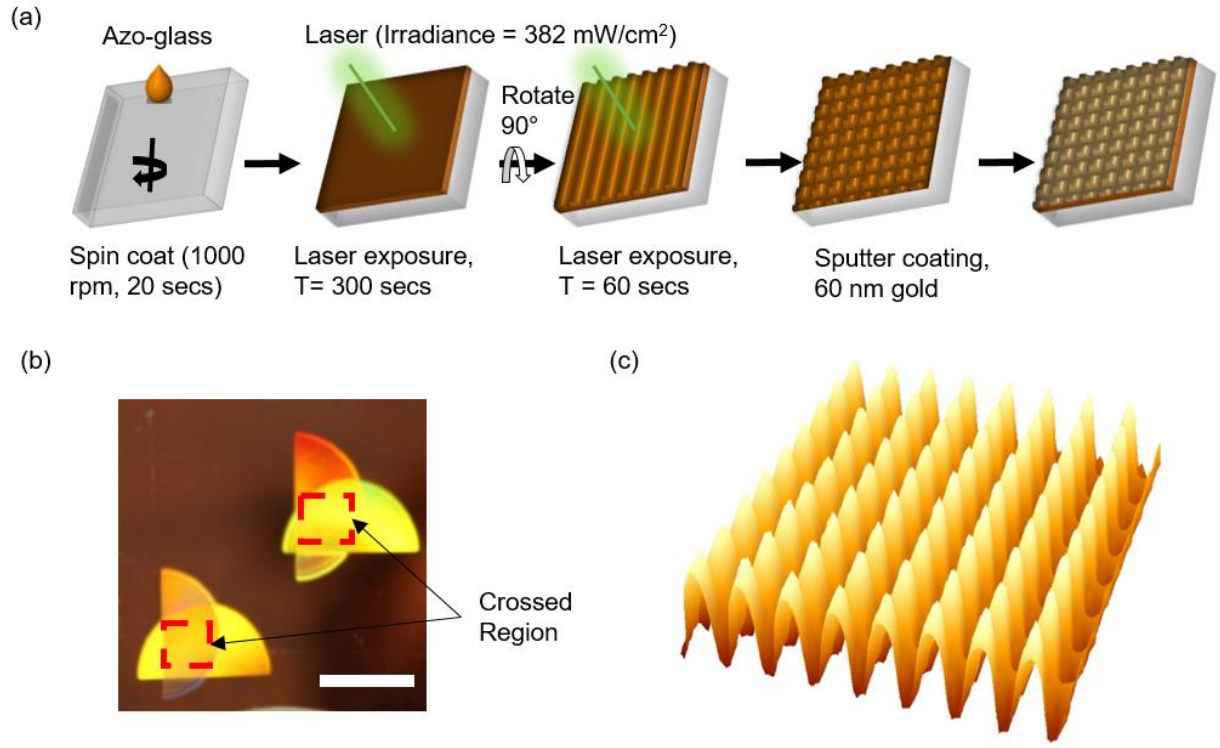

Figure 1. Azobenzene molecular glass based cross-grating structures. a. Schematics for fabrication of cross gratings. b. Fabricated cross-grating structures with 550-nm pitch (Scale bar = 1 cm). c. Atomic Force Microscopy scan of the crossed region (scan size: 10 μm x 10 μm).

.

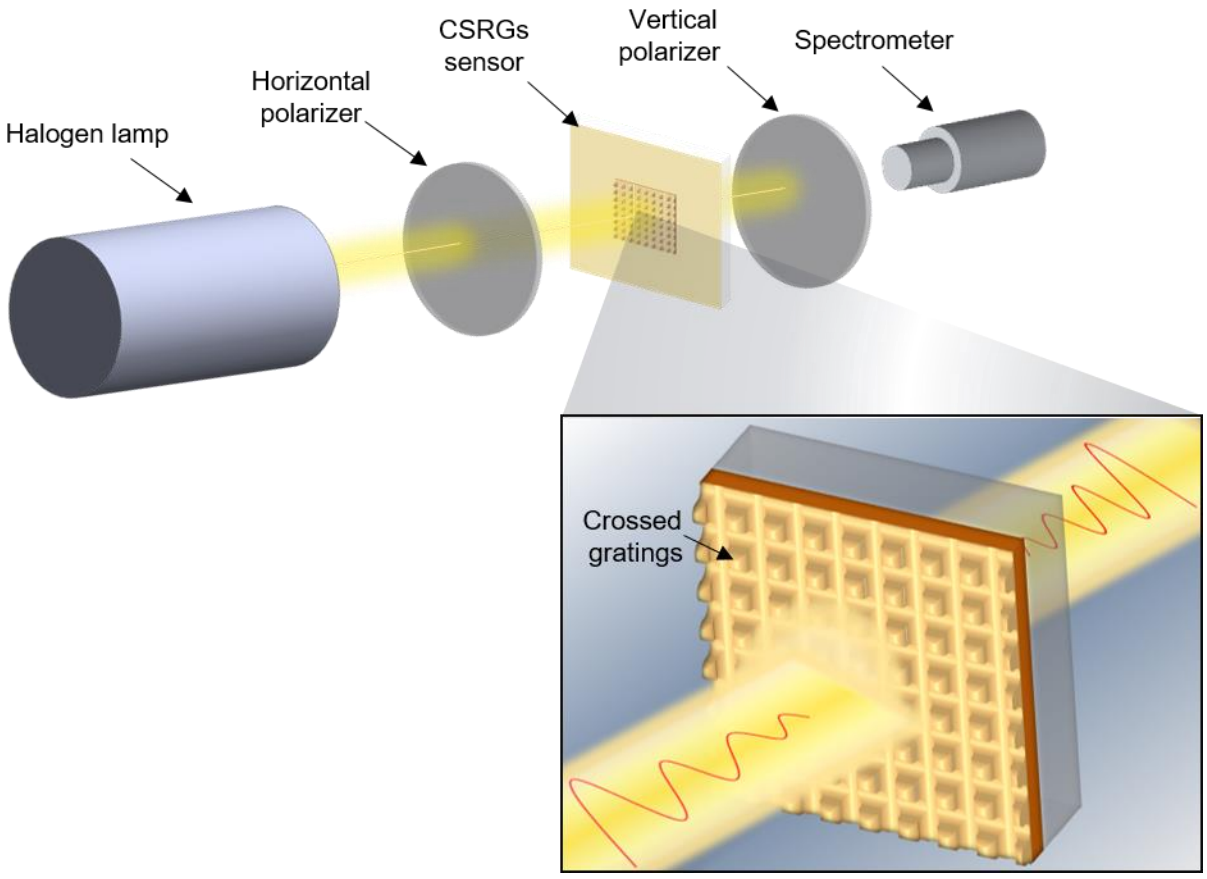

Figure 2. Schematic of the optical setup for transmission-based spectroscopy using CSRGs. All the components are placed in a collinear arrangement. The light from a halogen lamp passes through a horizontal polarizer, and is incident on the CSRGs exciting the plasmons in two levels. The resulting out-coupled light then passes through the vertical polarizer, eliminating all residual light from the halogen lamp, except the plasmonic signal detected by the spectrometer.

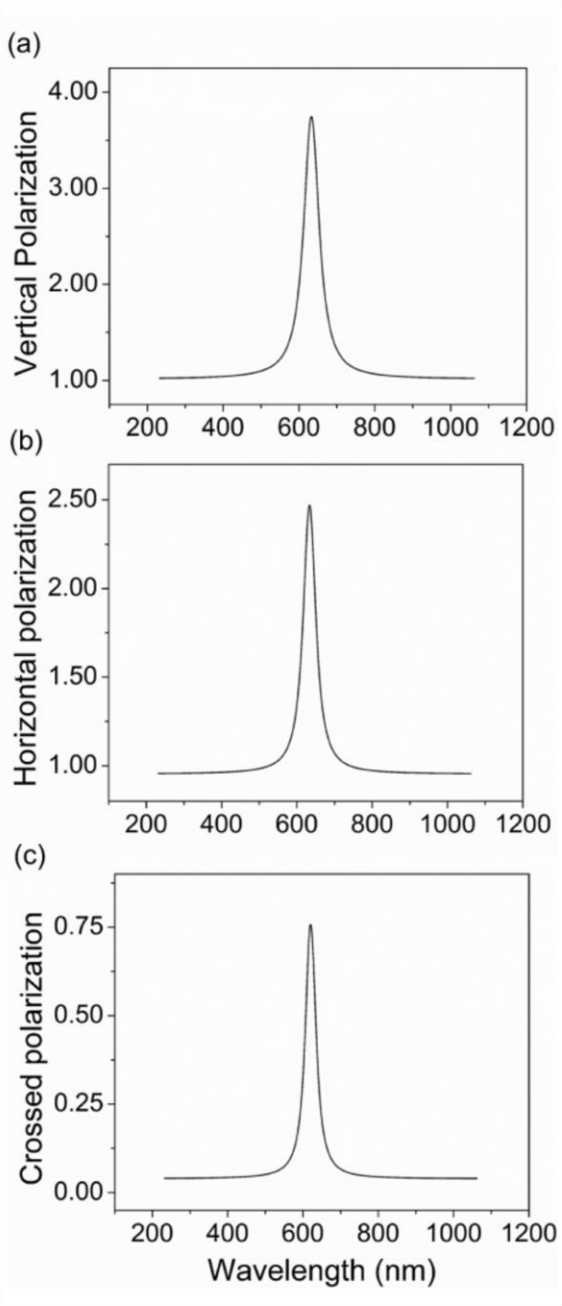

Figure 3. Normalized transmission spectra of the crossed region obtained by dividing transmission spectra for (a) first polarizer vertical and second polarizer removed (b) first polarizer horizontal and second polarizer removed and (c) first polarizer horizontal and second polarizer vertical by the gold/azo-glass absorption spectra from an area where there is no grating.

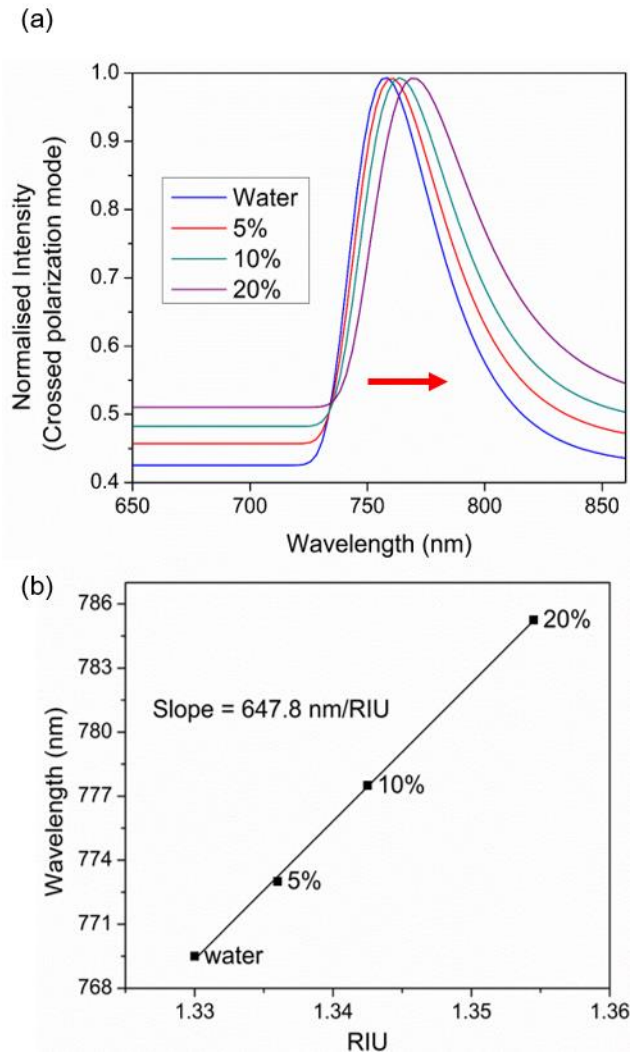

Figure 4. Bulk Sensitivity test. (a) Normalized SPR peaks for water and sucrose solutions of different concentrations (5%, 10% and 20%). Red shift is observed as the concentration i.e. refractive index of solution increases. (b) Due to the similar shape of the curves, wavelength corresponding to 90% intensity after the SPR peaks is considered for measuring the sensitivity. Wavelength (nm) vs refractive index (RIU) of each solutions results in a linear sensitivity curve with slope i.e. sensitivity= 647.8 nm/RIU. No error bars are indicated since the standard deviation for N = 3 is smaller than the size of the symbol representing the mean in the graph.

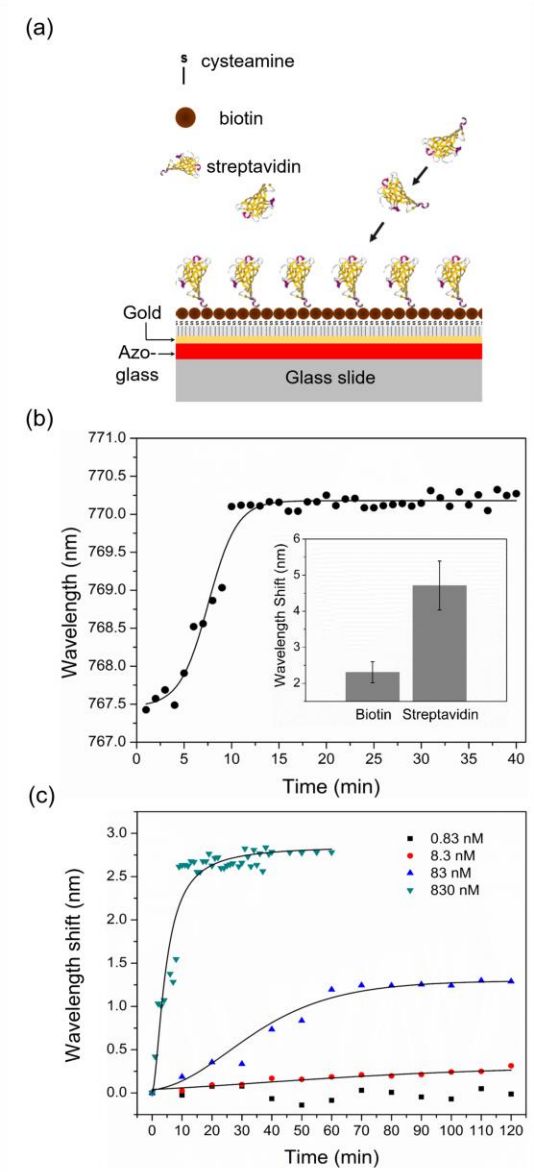

Figure 5. Time-dependent streptavidin detection assay. (a) Schematics of streptavidin-biotin-cysteamine complex on the nanoplasmonic sensors. (b) Observed λ_{SPR} value versus streptavidin incubation time at 830 nM concentration. The inset shows the cumulative shift in λ_{SPR} observed after addition of biotin and streptavidin to the cysteamine SAM system with error bars showing the standard deviation from the mean observed shift (N = 2). (c) Dose-dependent binding study at 0.83, 8.3, 83 and 830 nM streptavidin concentrations. The plot shows the real-time λ_{SPR} peak shift over the incubation period.

REFERENCES

(1) Sonato, A.; Agostini, M.; Ruffato, G.; Gazzola, E.; Liuni, D.; Greco, G.; Travagliati, M.; Cecchini, M.; Romanato, F. Lab on a Chip A Surface Acoustic Wave (SAW)-Enhanced Grating- Coupling Phase-Interrogation Surface Plasmon Resonance (SPR) Microfluidic Biosensor. *Lab Chip* **2016**, *16*, 1224–1233.

(2) Valsecchi, C.; Brolo, A. G. Periodic Metallic Nanostructures as Plasmonic Chemical Sensors. *Langmuir* **2013**, *29*, 5638–5649.

(3) Spadavecchia, J.; Barras, A.; Lyskawa, J.; Woisel, P.; Laure, W.; Pradier, C.-M.; Boukherroub, R.; Szunerits, S. Approach for Plasmonic Based DNA Sensing: Amplification of the Wavelength Shift and Simultaneous Detection of the Plasmon Modes of Gold Nanostructures. *Anal. Chem.* **2013**, *85*, 3288–3296.

(4) Im, H.; Lee, S. H.; Wittenberg, N. J.; Johnson, T. W.; Lindquist, N. C.; Nagpal, P.; Norris, D. J.; Oh, S.-H. Template-Stripped Smooth Ag Nanohole Arrays with Silica Shells for Surface Plasmon Resonance Biosensing. *ACS Nano* **2011**, *5*, 6244–6253.

(5) Junesch, J.; Sannomiya, T.; Dahlin, A. B. Optical Properties of Nanohole Arrays in Metal–Dielectric Double Films Prepared by Mask-on-Metal Colloidal Lithography. *ACS Nano* **2012**, *6*, 10405–10415.

(6) Chan, W. C. W.; Udugama, B.; Kadhiresan, P.; Kim, J.; Mubareka, S.; Weiss, P. S.; Parak, W. J. Patients, Here Comes More Nanotechnology. *ACS Nano* **2016**, *10*, 8139–8142.

(7) Wang, Y.; Knoll, W.; Dostalek, J. Bacterial Pathogen Surface Plasmon Resonance Biosensor Advanced by Long Range Surface Plasmons and Magnetic Nanoparticle Assays. *Anal. Chem.* **2012**, *84*, 8345–8350.

(8) Ravindranath, S. P.; Mauer, L. J.; Deb-Roy, C.; Irudayaraj, J. Biofunctionalized Magnetic Nanoparticle Integrated Mid-Infrared Pathogen Sensor for Food Matrixes. *Anal. Chem.* **2009**, *81*, 2840–2846.

(9) Vaisocherová-lísalová, H.; Ví, I.; Laura, M.; Chadtová, X.; Mrázek, J.; Lama, J.; Lynn, N. S.; Petr, Š. Biosensors and Bioelectronics Low-Fouling Surface Plasmon Resonance Biosensor for Multi-Step Detection of Foodborne Bacterial Pathogens in Complex Food Samples. **2016**, *80*, 84–90.

(10) Forzani, E. S.; Foley, K.; Westerhoff, P.; Tao, N. Detection of Arsenic in Groundwater Using a Surface Plasmon Resonance Sensor. *Sensors Actuators, B Chem.* **2007**, *123*, 82–88.

(11) Homola, J. Surface Plasmon Resonance Sensors for Detection of Chemical and Biological Species. *Chem. Rev.* **2008**, *108*, 462–493.

(12) Teh, H. F.; Peh, W. Y. X.; Su, X.; Thomsen, J. S. Characterization of Protein-DNA Interactions Using Surface Plasmon Resonance Spectroscopy with Various Assay Schemes. *Biochemistry* **2007**, *46*, 2127–2135.

(13) Escobedo, C.; Chou, Y.-W.; Rahman, M.; Duan, X.; Gordon, R.; Sinton, D.; Brolo, A. G.; Ferreira, J. Quantification of Ovarian Cancer Markers with Integrated Microfluidic Concentration Gradient and Imaging Nanohole Surface Plasmon Resonance. *Analyst* **2013**, *138*, 1450–1458.

(14) Aćimović, S. S.; Ortega, M. A.; Sanz, V.; Berthelot, J.; Garcia-Cordero, J. L.; Renger, J.; Maerkl, S. J.; Kreuzer, M. P.; Quidant, R. LSPR Chip for Parallel, Rapid, and Sensitive Detection of Cancer Markers in Serum. *Nano Lett.* **2014**, *14*, 2636–2641.

(15) Hemmi, A.; Usui, T.; Moto, A.; Tobita, T.; Soh, N.; Nakano, K.; Zeng, H.; Uchiyama, K.; Imato, T.; Nakajima, H. A Surface Plasmon Resonance Sensor on a Compact Disk-Type Microfluidic Device. *J. Sep. Sci.* **2011**, *34*, 2913–2919.

(16) Xu, B.-B.; Ma, Z.-C.; Wang, H.; Liu, X.-Q.; Zhang, Y.-L.; Zhang, X.-L.; Zhang, R.; Jiang, H.-B.; Sun, H.-B. A SERS-Active Microfluidic Device with Tunable Surface Plasmon Resonances. *Electrophoresis* **2011**, *32*, 3378–3384.

(17) Vala, M.; Chadt, K.; Piliarik, M.; Homola, J. High-Performance Compact SPR Sensor for Multi-Analyte Sensing. *Sensors Actuators B Chem.* **2010**, *148*, 544–549.

(18) Yeh, W.-H.; Kleingartner, J.; Hillier, A. C. Wavelength Tunable Surface Plasmon Resonance-Enhanced Optical Transmission Through a Chirped Diffraction Grating. *Anal. Chem.* **2010**, *82*, 4988–4993.

(19) Bhatta, D.; Stadden, E.; Hashem, E.; Sparrow, I. J. G.; Emmerson, G. D. Multi-Purpose Optical Biosensors for Real-Time Detection of Bacteria, Viruses and Toxins. *Sensors Actuators B Chem.* **2010**, *149*, 233–238.

(20) Rochon, P.; Batalla, E.; Natansohn, A. Optically Induced Surface Gratings on Azoaromatic Polymer Films. *Appl. Phys. Lett.* **1995**, *66*, 136–138.

(21) Kim, D. Y.; Tripathy, S. K.; Li, L.; Kumar, J. Laser-Induced Holographic Surface Relief Gratings on Nonlinear Optical Polymer Films. *Appl. Phys. Lett.* **1995**, *66*, 1166–1168.

(22) Homola, J. *Surface Plasmon Resonance Based Sensors*; Springer: Berlin, 2006; Vol. 4.

(23) Barnes, W. L.; Dereux, A.; Ebbesen, T. W. Surface Plasmon Subwavelength Optics. *Nature* **2003**, *424*, 824–830.

(24) Bryan-Brown, G. P.; Sambles, J. R.; Hutley, M. C. Polarisation Conversion through the Excitation of Surface Plasmon on a Metallic Grating. *J. Mod. Opt.* **1990**, *37*, 1227–1232.

(25) Watts, R. A.; Harris, J. B.; Hibbins, A. P.; Preist, T. W.; Sambles, J. R. Optical Excitation of Surface Plasmon Polaritons on 90° and 60° Bi-Gratings. *J. Mod. Opt.* **1996**, *43*, 1351–1360.

(26) Sabat, R. G.; Rochon, N.; Rochon, P. Dependence of Surface Plasmon Polarization Conversion on the Grating Pitch. *J. Opt. Soc. Am. A* **2010**, *27*, 518–522.

(27) Jefferies, J.; Sabat, R. G. Surface-Relief Diffraction Gratings' Optimization for Plasmonic

Enhancements in Thin-Film Solar Cells. *Prog. Photovoltaics Res. Appl.* **2014**, *22*, 648–655.

(28) Kirby, R.; Sabat, R. G.; Nunzi, J.-M.; Lebel, O. Disperse and Disordered: A Mexylaminotriazine-Substituted Azobenzene Derivative with Superior Glass and Surface Relief Grating Formation. *J. Mater. Chem. C* **2014**, *2*, 841–847.

(29) Monteiro, J. P.; Ferreira, J.; Sabat, R. G.; Rochon, P.; Santos, M. J. L.; Girotto, E. M. SPR Based Biosensor Using Surface Relief Grating in Transmission Mode. *Sensors Actuators, B Chem.* **2012**, *174*, 270–273.

(30) Kumawat, N.; Pal, P.; Varma, M.; Fan, X.; Okumoto, S.; Jones, A.; Frommer, W. B.; Taitt, C. R.; Anderson, G. P.; Ligler, F. S.; *et al.* Diffractive Optical Analysis for Refractive Index Sensing Using Transparent Phase Gratings. *Sci. Rep.* **2015**, *5*, 16687.

(31) Henzie, J.; Lee, M. H.; Odom, T. W. Multiscale Patterning of Plasmonic Metamaterials. *Nat. Nanotechnol.* **2007**, *2*, 549–554.

(32) Escobedo, C.; Brolo, A. G.; Gordon, R.; Sinton, D. Optofluidic Concentration: Plasmonic Nanostructure as Concentrator and Sensor. *Nano Lett.* **2012**, *12*, 1592–1596.

(33) Yanik, A. A.; Huang, M.; Artar, A.; Chang, T. Y.; Altug, H. Integrated Nanoplasmonic-Nanofluidic Biosensors with Targeted Delivery of Analytes. *Appl. Phys. Lett.* **2010**, *96*, 21101.

(34) Squires, T. M.; Messinger, R. J.; Manalis, S. R. Making It Stick: Convection, Reaction and Diffusion in Surface-Based Biosensors. *Nat. Biotechnol.* **2008**, *26*, 417–426.

(35) Escobedo, C.; Vincent, S.; Choudhury, a I. K.; Campbell, J.; Brolo, a G.; Sinton, D.; Gordon, R. Integrated Nanohole Array Surface Plasmon Resonance Sensing Device Using a Dual-Wavelength Source. *J. Micromechanics Microengineering* **2011**, *21*, 115001.

(36) Acímovic, S. S.; Ortega, M. A.; Sanz, V.; Berthelot, J.; Garcia-Cordero, J. L.; Renger, J.; Maerkl, S. J.; Kreuzer, M. P.; Quidant, R. LSPR Chip for Parallel, Rapid, and Sensitive Detection of Cancer Markers in Serum. *Nano Lett.* **2014**, *14*, 2636–2641.

(37) De Leebeeck, A.; Swaroop Kumar, L. K.; De Lange, V.; Sinton, D.; Gordon, R.; Brolo, A. G. On-Chip Surface-Based Detection with Nanohole Arrays. *Anal. Chem.* **2007**, *79*, 4096–4100.

(38) Marinakos, S. M.; Chen, S.; Chilkoti, A. Plasmonic Detection of a Model Analyte in Serum by a Gold Nanorod Sensor. *Anal. Chem.* **2007**, *79*, 5278–5283.

(39) Liu, B.; Wang, M.; He, Y.; Wang, X. Duplication of Photoinduced Azo Polymer Surface-Relief Gratings through a Soft Lithographic Approach. *Langmuir* **2006**, *22*, 7405–7410.

(40) Liedtke, A.; Lei, C.; O'Neill, M.; Dyer, P. E.; Kitney, S. P.; Kelly, S. M. One-Step Photoembossing for Submicrometer Surface Relief Structures in Liquid Crystal Semiconductors. *ACS Nano* **2010**, *4*, 3248–3253.

TABLE OF CONTENTS GRAPHIC: